

Abstract

The extrudate swell, the geometrical modifications that take place when the flowing material leaves the confined flow inside a channel and moves freely without the restrictions promoted by the walls, is a relevant phenomenon in several polymer processing techniques. For instance, in profile extrusion, the extrudate cross-section suffers a number of distortions motivated by swell, which are very difficult to anticipate, especially for complex geometries. As happens in many industrial processes, numerical modelling might provide useful information to support design tasks, enabling to identify the best strategy to compensate the changes promoted by the extrudate swell. There are different ways to model free-surface flows, which can be grouped in Interface Tracking (IT) and Interface Capturing (IC) approaches. When dealing with steady state processes, which is the case of profile extrusion, IT is usually the best alternative, since it does not present the problems related to interface diffusion inherent to the IC approaches.

OpenFOAM comprises a solver to simulate free-surface flows following an IT approach, which was proposed by Tukovic & Jasak (2008) and Tukovic *et al.*, (2012). This work aims to assess the capability of that solver to simulate the extrudate swell process in profile extrusion, by using the interfaceTrackingFvMesh and interTrackMeshMotion libraries available in OpenFOAM-v1912 to track the free surface movement with a dynamic mesh motion. For this purpose, the data provided by Mitsoulis *et al.*, (2012) on simulation of the extrudate swell of a Newtonian fluid at different Reynolds number flows is considered as the reference for validation.

Governing equations

The continuity and momentum equations for the isothermal flow of an incompressible Newtonian fluid inside a volume V bounded by a surface S :

$$\oint_S \mathbf{n} \cdot (\mathbf{u} - \mathbf{u}_s) dS = 0,$$

$$\frac{d}{dt} \int_V \rho \mathbf{u} dV + \oint_S \mathbf{n} \cdot \rho (\mathbf{u} - \mathbf{u}_s) \mathbf{u} dS = \oint_S \mathbf{n} \cdot (\mu \nabla \mathbf{u}) dS - \int_V \nabla p dV,$$

\mathbf{n} : unit normal vector on S , ρ : the fluid density, \mathbf{u} : the fluid velocity,

\mathbf{u}_s : the surface S velocity, μ : the fluid dynamic viscosity,

p : the dynamic pressure $p = p_{abs} - p_{hydrostatic}$, $p_{hydrostatic} = \rho \mathbf{g} \cdot \mathbf{r}$,

\mathbf{g} : gravitational acceleration, \mathbf{r} : the position vector.

The mathematical model, valid for arbitrary moving volume, is obtained from the corresponding material volume model using the Reynolds' transport theorem [Tukovic & Jasak (2012)]. The mesh deformation is used to calculate the interface position, following an IT approach, the relation between the rate of change of the volume V and the surface velocity \mathbf{u}_s is defined by the *space conservation law* [Demirdžić & Perić (1988)]:

$$\frac{d}{dt} \int_V dV - \oint_S \mathbf{n} \cdot \mathbf{u}_s dS = 0.$$

This approach called arbitrary Lagrangian-Eulerian formulation (ALE) [Tukovic & Jasak (2008)].

Force balance at the free surface

Dynamic condition: from the momentum conservation law, the forces acting at the fluid interface must be in equilibrium between two fluids; subscripts 1 and 2 (see Fig 1).

$$\mathbf{n} \cdot \mathbf{T}_1 - \mathbf{n} \cdot \mathbf{T}_2 = \sigma (\nabla_s \cdot \mathbf{n}) \mathbf{n} - \nabla_s \sigma$$

stress tensors: $\mathbf{T}_1 = -p_1 \mathbf{I} + \mu_1 [\nabla \mathbf{u}_1 + (\nabla \mathbf{u}_1)^T]$, $\mathbf{T}_2 = -p_2 \mathbf{I} + \mu_2 [\nabla \mathbf{u}_2 + (\nabla \mathbf{u}_2)^T]$,

tangential gradient operator: $\nabla_s = [\mathbf{I} - \mathbf{nn}] \cdot \nabla = \nabla - \mathbf{n} \frac{\partial}{\partial n}$

surface tension: σ . Mean curvature: $\kappa = \nabla_s \cdot \mathbf{n} = \frac{1}{R_1} + \frac{1}{R_2}$,

the *dynamic boundary condition* can be generally written as:

$$[\mathbf{T}_2 - \mathbf{T}_1] \cdot \mathbf{n} = \nabla_s \sigma - \sigma \kappa \mathbf{n}.$$

Normal force balance: $\mathbf{n} \cdot \{[\mathbf{T}_2 - \mathbf{T}_1] \cdot \mathbf{n}\} = -\sigma \kappa$

after some algebra, pressure jump condition is obtained:

$$p_2 - p_1 = \sigma \kappa - 2(\mu_2 - \mu_1) \nabla_s \cdot \mathbf{u}, \quad (1)$$

Tangential force balance: $\mathbf{t} \cdot \{[\mathbf{T}_2 - \mathbf{T}_1] \cdot \mathbf{n}\} = \mathbf{t} \cdot (\nabla_s \sigma)$

After some algebra and discretizing, the tangential velocity at the face $1f$ is obtained:

$$(\mathbf{u}_{1f})_t = (\mathbf{u}_{1c})_t + \frac{(\nabla_s \sigma)_{1f} + (\mu_2 - \mu_1) (\nabla_s u_n)_{1f}}{\frac{\mu_1}{(\delta_{1f})_n}}. \quad (2)$$

After some algebra, the normal velocity to face $1f$ is calculated

$$\mathbf{n}_{1f} \cdot (\nabla \mathbf{u})_{1f} = \frac{(\nabla_s \sigma)_{1f} - \mathbf{n}_{1f} (\nabla_s \cdot \mathbf{u})_{1f} - (\nabla_s \mathbf{u})_{1f} \cdot \mathbf{n}_{1f}}{\mu_1} \quad (3)$$

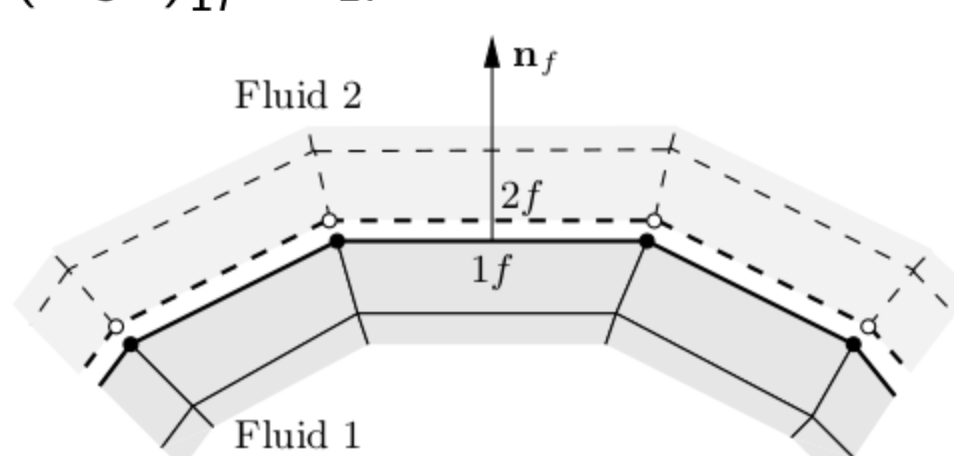


Fig 1. The interface shown by Tukovic & Jasak (2008)

The interTrackMeshMotion for the free surface

Generally after an outer iteration, the net mass flux through the boundary side f at the interface, i.e. $\dot{m}_{1f} - \rho_1 \dot{V}_{1f} \neq 0$

Where \dot{m}_{1f} is the mass flux through the face $1f$ and $\dot{V}_{1f} = \frac{3 \delta V_f^p}{2 \Delta t} - \frac{1 \delta V_f^{p-1}}{2 \Delta t}$ is the cell face volume flux at face $1f$ (at current time step n) which is obtained to satisfy discretized geometric conservation law, δV_f^p is the volume swept by the cell face f while moving $V_f^p - V_f^{p-1} = \sum_f \delta V_f^p$.

Therefore, points must be moved for volume flux corrections: $\dot{V}_{1f} = \dot{m}_{1f} / \rho_1 - \dot{V}_{1f}$.

- The interface points displacements based on Muzaferija & Perić (1997): a control point $1c$ attached to $1f$ is moved to cancel the net mass flux (see Fig 2).
- The interface mesh point $1i$ is moved up to a plane laid over the corresponding control points with an accurate interpolation.
- The internal nodes need to be moved according to the solution of solving a Laplacian equation

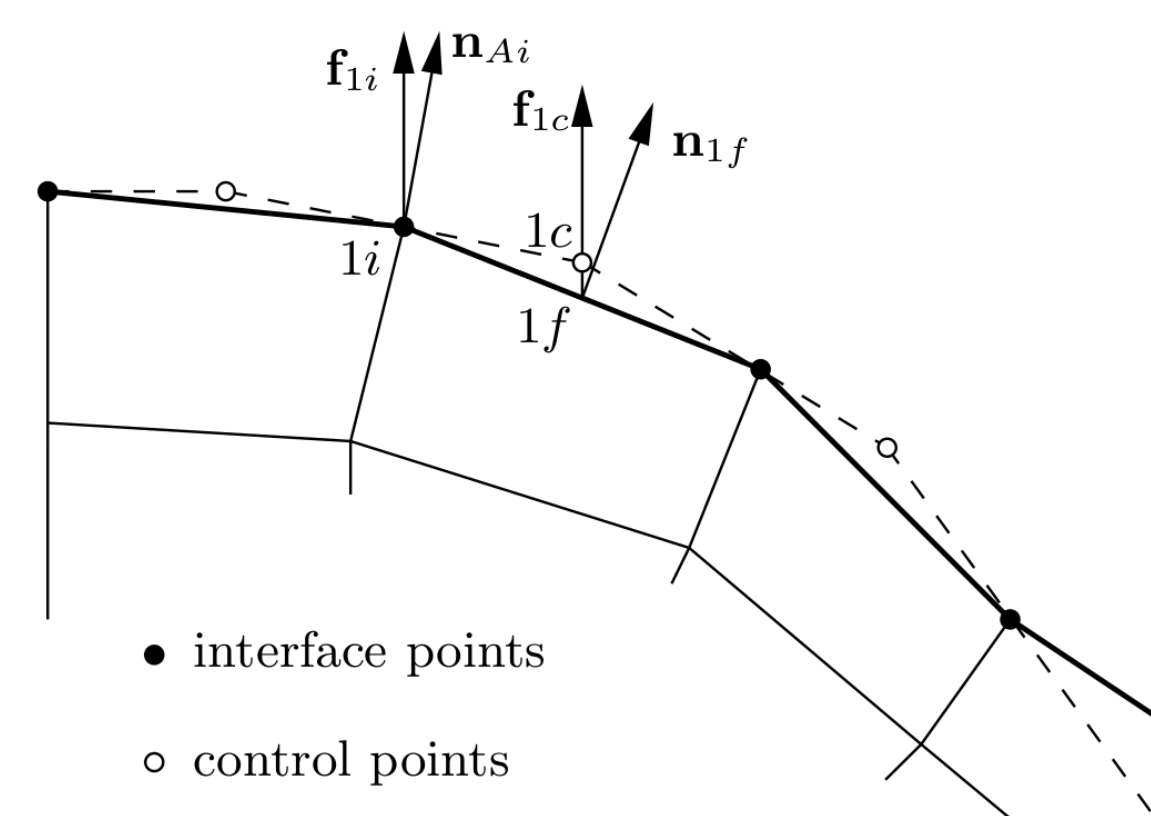


Fig 2. The interface mesh movement by Tukovic & Jasak (2008)

The interfaceTrackingFvMesh for the free surface

interfaceTrackingFvMesh enables using freeSurfaceVelocity and freeSurfacePressure boundary conditions. Here is the sequence of calculations at the free surface [Tukovic & Jasak (2012)]:

- 1) Tangential component of the free surface velocity \mathbf{u}_{1f} is calculated from tangential force balance (2),
- 2) The normal velocity derivative specified at $1f$ is computed using updated surface velocity (3),
- 3) The value of dynamic pressure is computed from the pressure jump (1).

Computational domain and the boundary conditions

A schematic of the domain and the boundary conditions are shown in Fig 3.

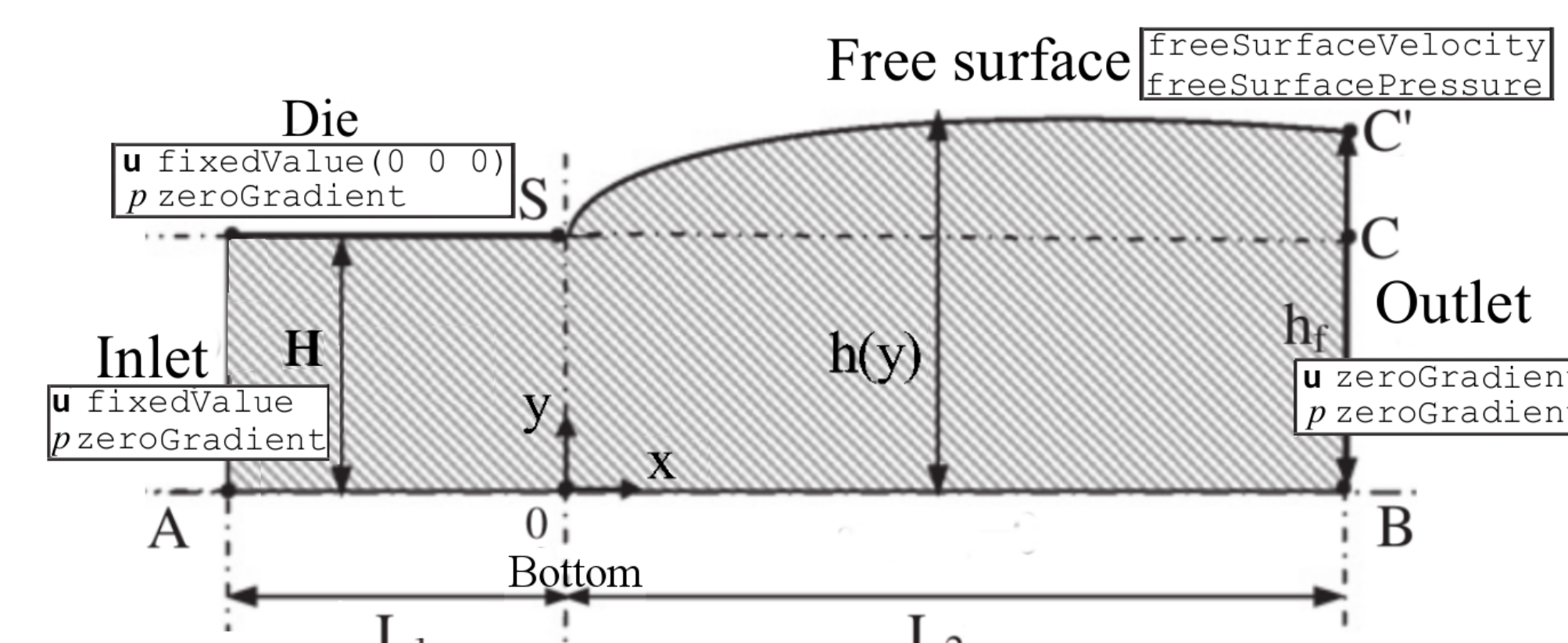


Fig 3. A schematic of the extrusion process by Mitsoulis *et al.*, (2012)

For planar case: frontAndBack: empty

For axis-symmetric case: front: wedge back: wedge Bottom: empty

$L_1 = 5$ mm, $L_2 = 25$ mm, $H = 1$ mm, simulation starting from $Re = \rho U_{mean} H / \mu = 0.1$.

Simulation settings

interfaceTrackingFvMesh and interTrackMeshMotion libraries are called in controlDict, pimpleFoam solver is used. A maximum Courant number of 0.2 is employed for the simulations.

For the transient term the Euler discretization scheme is employed, while for spatial discretization terms Gauss linear approximations were used mostly.

Grid sensitivity analysis

A grid requirement test is carried out for validation of extrudate swell ratio (which is the height of the free surface at the outlet divided by the die height) of Newtonian fluid at $Re=0.1$. The grids for resolution test are stretched in x, y with an $AR=0.4$ to have the maximum resolution downstream of the die.

Table 1. Different meshes tested

	M1	M2	M3	M4
NxNy	320x37	480x56	720x84	1080x126
DOF (total cells * total variables)	47360	107520	241920	544320

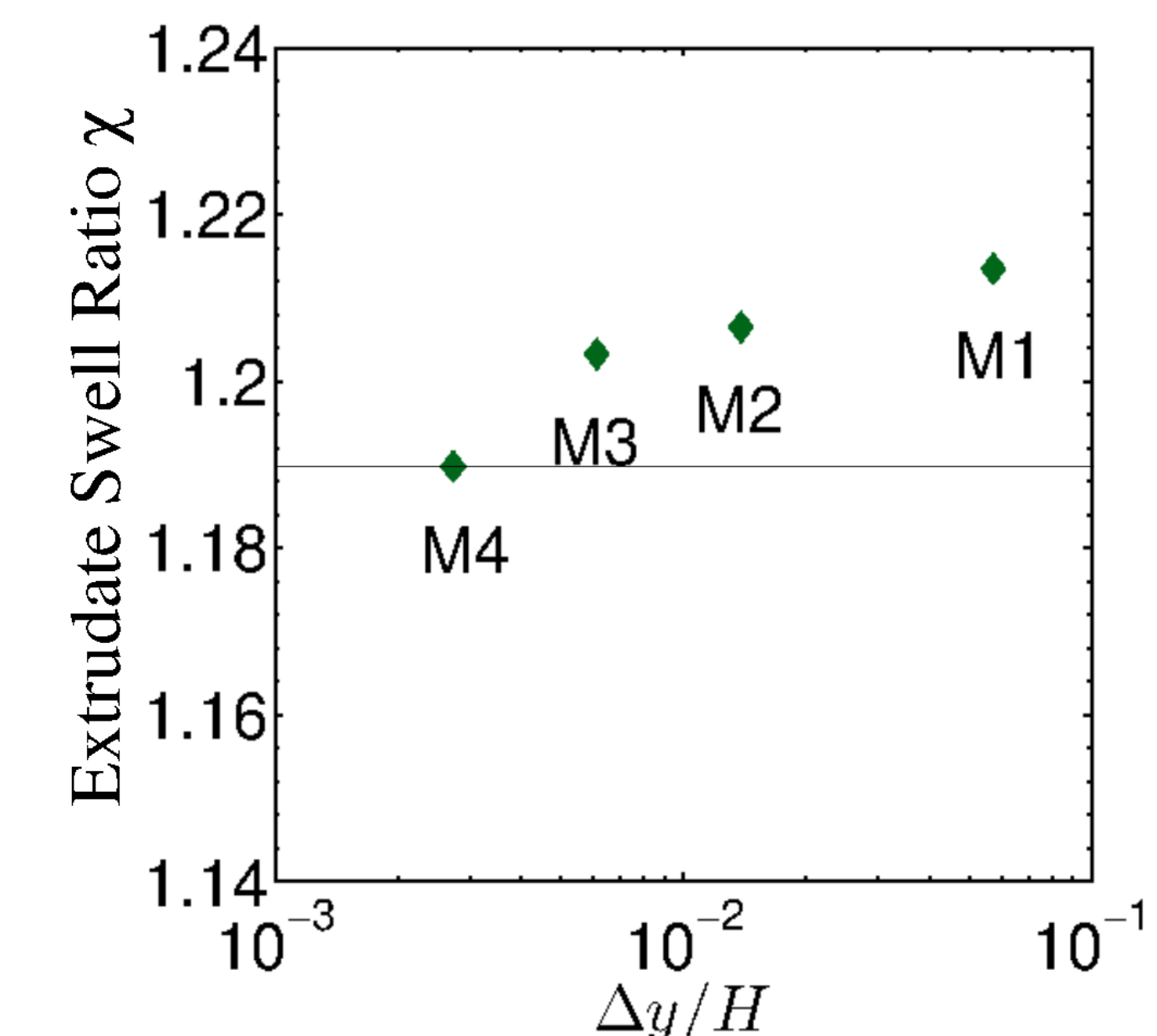


Fig 4. Extrudate swell ratio for different grids at $Re=0.1$ (reference value ~ 1.19).

The mesh M4 is used for the simulations at different Reynolds numbers for validation.

Results

The simulations are carried out at different Reynolds numbers from 0.1 to 10, and the extrudate swell ratio is compared with the reference data by Mitsoulis *et al.*, (2012)

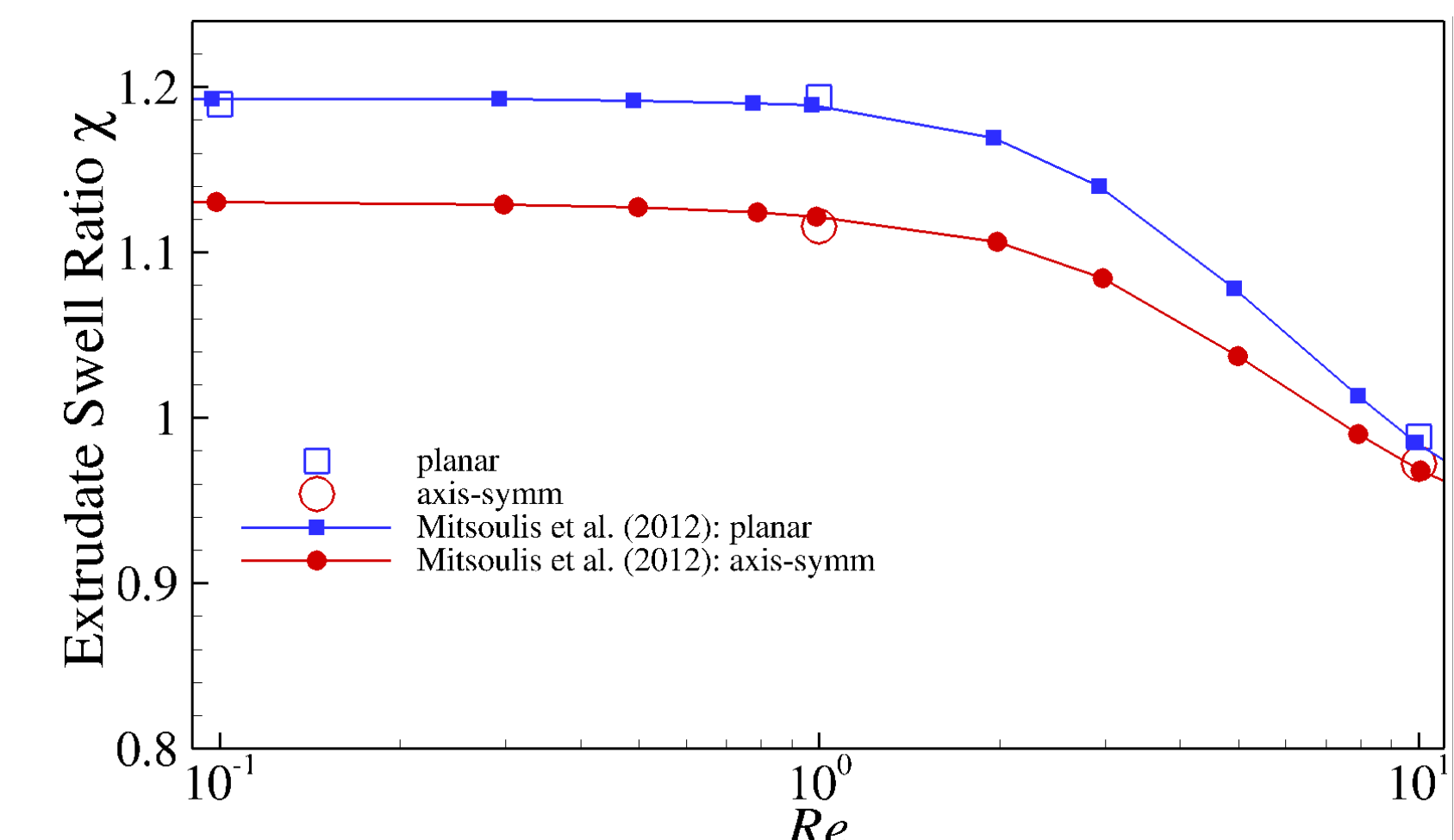


Fig 5. Extrudate swell ratio of Newtonian fluid compared with Mitsoulis *et al.*, (2012)

Conclusion and future work

The solver is being validated for $Re=0.1, 1, 10$ for the simulation of extrusion process of a Newtonian fluid.

The next steps are to include a more realistic rheological model for optimization of the die and to apply the solver to support the design of profile extrusion dies.

Acknowledgement

The authors would like to acknowledge the funding by FEDER funds through the COMPETE 2020 Programme and National Funds through FCT - Portuguese Foundation for Science and Technology under the projects UIDB/05256/2020 and UIDP/05256/2020, TSSIPRO - Technologies for Sustainable and Smart Innovative Products (NORTE-01-0145-FEDER-000015) and FAMEST - Footwear, Advanced Materials, Equipment's and Software Technologies (POCI-01-0247-FEDER-024529). The authors also acknowledge the support of the computational clusters Search-ON2 (NORTE-07-0162-FEDER-000086) and Minho Advanced Computing Center (MACC).

References

- Z. Tukovic and H. Jasak, 2008. Simulation of free-rising bubble with soluble surfactant using moving mesh finite volume/area method. *In 6th International Conference on CFD in Oil & Gas, Metallurgical and Process Industries*, Trondheim, Norway.
- Z. Tukovic and H. Jasak, 2012. A moving mesh finite volume interface tracking method for surface tension dominated interfacial fluid flow. *Computers & Fluids*, 55:70-84.
- E. Mitsoulis, G. C. Georgiou, Z. Kountouriotis, 2012. A study of various factors affecting Newtonian extrudate swell. *Computers & Fluids*, 57:195-207.
- I. Demirdžić, M. Perić, 1988. Space conservation law in finite volume calculations of fluid flow, *International Journal for Numerical Methods in Fluids*, 8: 1037-1050
- S. Muzaferija, M. Perić, 1997. Computation of free surface flows using the finite-volume method and moving grids, *Numerical heat transfer, Part B: Fundamentals* 32: 369-384.